Cyclic Oxidation of P91 at 1073, 1123 and 1173 K

S. Rajendran Pillai*, P. Sankar# and H.S. Khatak*

**Corrosion Science and Technology Division, # Physical Metallurgy Section*
Materials Characterization Group, Indira Gandhi Centre for Atomic Research
Kalpakkam, Tamil Nadu, India-603 102

(Received December 16, 2003; final form February 10, 2004)

ABSTRACT

Cyclic oxidation behaviour of modified 9Cr-1Mo steel has been investigated under three temperatures of 1073, 1123 and 1173 K. The adherence characteristics of the scale were studied by the 'transient mass gain' method by employing a thermogravimetric balance. A cycle time of 7.2 ks (2 h) was employed and at each temperature the specimen was oxidised for 360 ks (100 h, 50 cycles). Experiments revealed that the scale is mostly adherent in an isothermal condition. However, on cooling, the thermal expansion differential between the oxide scale and the parent alloy caused the development of cracks leading to spallation. The threshold thickness of the scale for the initiation of cracks and spallation was evaluated. Post-oxidation examinations were carried out by using XRD, SEM and EDS. Oxides of the type Fe_2O_3, $FeCr_2O_4$ were predominant at the surface at 1123 and 1173 K. At the relatively lower temperature of 1073 K, in addition to the above oxides, the scale also contained Cr_2O_3. The interspace of the oxide/alloy also contained significant amounts of oxide of chromium. The reason for such distribution of oxide phases has been explained by invoking thermodynamic and diffusion concepts.

1. INTRODUCTION

Modified grade of 9Cr-1Mo steel (referred to as P91) finds application in high temperature environment because of the combined advantages of good creep strength and resistance to water induced stress corrosion cracking. This alloy finds application in fast reactors in the fabrication of steam generator and decay heat removal systems. One of the major limitations of this alloy is the ready oxidation of the constituent elements (iron, chromium and molybdenum) at higher temperature. If the oxide scale formed initially is adherent, the further advancement of the oxidation may be retarded. Further progress in the oxidation will be governed by a diffusion-controlled parabolic rate law. On the other hand, if the integrity of the scale is poor, characterized by occasional cracking and spallation, then fresh surface will be exposed to oxygen at intermittent intervals so that oxidation can proceed unabated. Such a situation can lead to considerable loss in the thickness of the material that has to be accounted at the design stage itself (in terms of thickness loss) to impart adequate life to the components. The integrity of the scale is affected due to the process of growth itself predominantly on account of the increase in volume associated with oxidation. Besides, the operation condition of the component such as temperature cycling and mechanical vibration would directly affect the integrity of the scale /1-10/.

In most applications of the high temperature alloys, the components are subjected to repeated heating and cooling cycles. Thus the integrity of the component is determined by the capacity of the oxide scale to withstand rigours of temperature cycling. In the majority of the cases, the thermal expansion coefficient of the metal (or the alloy) is higher by 30-50% than that of the corresponding oxide created. Hence thermal cycling of the component would invariably lead to the development of stress. Mechanical deformation of the

scale through buckling, delamination or the development of wedge-type cracks would relieve this stress /11,12/. The mode of failure of the scale is governed by the relative strength of adhesion of the scale to the alloy substrate and the tensile strength of the scale itself. There will be an instantaneous generation of the scale on the spalled or cracked surface due to the exposure of fresh region. Thus, oxidation on the thermally cycled components would proceed with a very fast kinetics and the damage to the components cannot be predicted by normal corrosion law /13/. In engineering systems, components face thermal cycling and hence the corrosion allowance has to be estimated by simulating similar conditions in the laboratory.

The element responsible for generating adherent scale is specifically maintained at an optimum concentration in the alloy. Selective diffusion and oxidation of this element would continue to promote the generation of an adherent scale. For the same reason, in case the oxide scale is damaged through repetitive spallation, then the concentration of this specific element would be substantially reduced in the alloy. A stage would be reached when the concentration in the matrix is no longer adequate to generate a protective scale so that the alloy would undergo oxidation at a very fast rate. This is referred to as catastrophic oxidation /14, 15/. The useful service life of the component is completed at this juncture and any further operation may lead to failure /16/. It is desirable to know the threshold thickness of the oxide that leads to spallation and the threshold concentration of the alloy that preclude the possibility of generating an adherent oxide scale. The present experiment is directed at determining some of these vital parameters.

Apart from the total duration of oxidation, the cycle frequency also affects the integrity of the scale. However, there is no direct relation between cycle frequency and the failure criteria of the scale. Smialek /14/ reported that in Ni-40 Al a more severe mass loss rates were observed for 7.2 ks (20 h) cycle tests, followed by 50 hour cycle, than 3.6 ks (1 h) cycle for the same total duration of time. However, if the cycles were not repeated in the same pattern the mass loss rate was completely different. Thus, it is very difficult to fix a most desirable cycle frequency for an alloy rather it varies from alloy to alloy depending on thermophysical condition. It is appropriate to be aware of this factor and take adequate care in the operation of the components.

In the present investigation, cycle duration of 7.2 ks (2 h) was employed. The mass change associated with oxidation was determined by using a thermogravimetric balance. The mass gain associated with cracking and spallation (due to exposure of fresh surface for oxidation) was determined by 'transient mass gain' method. The cracking and spalling of the scale is also dictated by the thickness of the scale, which is already generated. The present experiment is aimed at determining the threshold thickness for the initiation of cracking of the scale. This would make it possible to determine the loss of thickness over a long period and reasonably estimate the thickness loss of components. Post-oxidation examinations were carried out by using XRD, SEM and EDS.

2. EXPERIMENTAL

Specimens of modified 9Cr-1Mo steel (2-mm thickness, 10-mm width and 20-mm length, chemical composition given in Table 1) were prepared from mill-annealed material. This was subjected to 'normalising' by heating at a temperature of 1353 K for 3.6 ks (1 h) followed by tempering by heating at 1013 K for 3.6 ks (1 h). These specimens were polished using successive grades of silicon carbide-coated paper to 10 μm finish. One of these specimens was employed for each temperature of oxidation. High temperature oxidation and the associated mass gain was determined using a thermogravimetric balance (Model SETSYS, M/s Setaram, France) This equipment has a sensitivity of 0.4 μg.

Initially a blank run (without specimen), with only the container of the specimen (the platinum crucible), introduced into the furnace, was carried out at the desired temperature of the experiment (1073 K in the first instance). Any drift in the equipment or mass loss was recorded for 7.2 ks (2 h). There was no measurable change in the mass indicating satisfactory blank conditions and negligible drift in the measuring system. The blank runs carried out at 1123 and 1173 K also yielded the same results.

Table 1
Chemical composition of P91

Element	Cr	Mo	V	Ni	Nb	Mn	Ti	C	P	Cu	Al	Fe
Content	8.7	0.9	0.15	0.03	0.046	0.4	<10	160	0.029	160	230	rest

The contents of C, Ti, Cu, and Al are expressed in PPM. Other elements are expressed in mass %

One of the specimens was taken in the platinum crucible. The crucible along with the specimen was hung into the thermobalance. This arrangement enabled the determination of the mass of the oxide adhering to the specimen as well as that has spallen during the experiment. The specimen was heated to the temperature of 1073 K at a rate of 0.5 K/s. It was maintained at this temperature for 7.2 ks (2 h). At the end of the heating cycle, the specimen was cooled at the rate of 0.4 K/s and ultimately brought to the room temperature. During the cooling process also the mass change was continuously monitored. A crack in the scale was determined by the 'transient mass gain method' (instantaneous mass gain associated with exposure of fresh surface due to opening of cracks or spallation). The specimen was taken out of the crucible and the mass of the spalled oxide (if it occurs) was determined separately.

The same specimen was loaded into the thermo-analytical balance and identical cycling experiments were repeated for a total of 25 cycles. At the end of 25 cycles the surface morphology of the specimen was examined by Scanning Electron Microscopy. Further oxidation was continued with the specimen for additional 25 cycles and the mass gain was determined in each case. At the end of a total of 50 cycles, the specimen was subjected to post-oxidation examination by Scanning Electron Microscopy, Energy Dispersive Spectrometry and X-ray Diffraction.

Similar to the above cases, oxidation experiments were carried out using separate specimens at 1123 and 1173 K and the scale was examined by the post-oxidation methods which are mentioned above.

3. RESULTS AND DISCUSSION

The results of the mass gain in each cycle are given in Table 2. Each cycle was expected to follow a unique growth kinetics determined by the damage undergone by the scale in the previous cooling cycle. Hence the cumulative mass change (for the complete 50 cycles) was not expected to follow any definite laws of kinetics. Significant change in the oxidation rate was observed in the first few cycles. Hence this data is given in Table 2. However, subsequent variation was sluggish and hence the rate constant for every 5 cycle only are included to compare the trend of oxidation.

Table 2
Mass gain due to oxidation and parabolic rate constant.

(a) 1073 K

Cycle No.	Mass gain ($mgmm^{-2}$)	Parabolic rate constant ($mg^2mm^{-4}s^{-1}$)	Factor of decrease compared to first cycle
1	0.0015	$3.13x10^{-10}$	-
2	0.0005	$3.5x10^{-11}$	8.9
3	0.0004	$2.2x10^{-11}$	$1.4x10^{1}$
4	0.0005	$3.5x10^{-11}$	8.9
5	0.0009	$1.13x10^{-10}$	2.8
10	0.0021	$6.13x10^{-10}$	$5.1x10^{-1}$
15	0.0021	$6.13x10^{-10}$	$5.1x10^{-1}$
20	0.0011	$1.68x10^{-10}$	1.9
25	0.0011	$1.68x10^{-10}$	1.9
30	0.0009	$1.13x10^{-10}$	2.8
35	0.0007	$6.8x10^{-11}$	4.6
40	0.0009	$1.13x10^{-10}$	2.8
45	0.0012	$2.0x10^{-10}$	1.6
50	0.0012	$2.0x10^{-10}$	1.6

(b) 1123 K

Cycle No.	Mass gain ($mgmm^{-2}$)	Parabolic rate constant ($mg^2mm^{-4}s^{-1}$)	Factor of decrease compared to first cycle
1	0.016	$3.52x10^{-8}$	-
2	0.0027	$1.01x10^{-9}$	$3.48x10^{1}$
3	0.0035	$1.7x10^{-9}$	$2.1x10^{1}$
4	0.0035	$1.7x10^{-9}$	$2.1x10^{1}$
5	0.0029	$1.17x10^{-9}$	$3.0x10^{1}$
10	0.0026	$9.38x10^{-10}$	$3.8x10^{1}$
15	0.0016	$3.52x10^{-10}$	$1.0x10^{2}$
20	0.0013	$2.34x10^{-10}$	$1.5 x10^{2}$
25	0.0009	$1.13x10^{-10}$	$3.1 x10^{2}$
30	0.0017	$4.01x10^{-10}$	$8.7 x10^{1}$
35	0.0013	$2.35x10^{-10}$	$1.5 x10^{2}$
40	0.0010	$1.39x10^{-10}$	$2.5 x10^{2}$
45	0.0007	$6.79x10^{-11}$	$5.1 x10^{2}$
50	0.0006	$4.98x10^{-11}$	$7.0 x10^{2}$

(c) 1173 K

Cycle No.	Mass gain ($mgmm^{-2}$)	Parabolic rate constant ($mg^2mm^{-4}s^{-1}$)	Factor of decrease compared to first cycle
1	0.107	$1.59x10^{-6}$	-
2	0.0294	$1.18x10^{-7}$	$1.3 x10^{1}$
3	0.0368	$1.89x10^{-7}$	8.4
4	0.0415	$2.39x10^{-7}$	6.7
5	0.0458	$2.91x10^{-7}$	5.5
10	0.0143	$2.84x10^{-8}$	$5.6 x10^{1}$
15	0.0043	$2.57x10^{-9}$	$6.19x10^{2}$
20	0.0053	$3.9x10^{-9}$	$4.08 x10^{2}$
25	0.0023	$7.35x10^{-10}$	$2.2 x10^{3}$
30	0.0023	$7.35x10^{-10}$	$2.2 x10^{3}$
35	0.0009	$1.13x10^{-10}$	$1.4 x10^{4}$
40	0.0012	$2.0x10^{-10}$	$7.9 x10^{3}$
45	0.0031	$1.33x10^{-9}$	$1.2 x10^{3}$
50	0.0032	$1.42x10^{-9}$	$1.1 x10^{3}$

3.1 Analysis of the trend in oxidation rate based on parabolic rate constant

The oxidation of the alloy at 1073 K showed the following characteristics.

(i) The rate showed a decrease by an order of magnitude in the 2-4 cycles when compared to the first cycle.

(ii) Subsequently the kinetics of oxidation became faster and attained a value amounting to double that of the first cycle for the cycle between 10-15.

(iii) The kinetics of oxidation remained lower than the initial cycle at a value of $2x10^{-10}$ $mg^2mm^{-4}s^{-1}$ at the subsequent cycles suggesting a constant growth rate on account of commendable integrity of the scale.

The main characteristics of the oxidation under 1123 K are;

(i) At this temperature the rate constants were 1-2 orders of magnitude higher than that at 1073 K.

(ii) As in the case at 1073 K, with progress of the number of cycles, the rate constant decreases. The decrease is nearly two orders of magnitude after attaining 15 cycles. Subsequently the oxidation rate is further lowered on account of the influence from the pre-existing oxide layer.

The main features of oxidation at 1173 K are;

(i) The initial rate of oxidation was substantially higher when compared to that at 1073 K and 1123 K. The rates were 2 orders of magnitude higher than the rate at 1123 K and 4 orders of magnitude higher than at 1073 K.

(ii) The rate showed a continuous decline at progressively higher cycles. The decrease was 3 orders of magnitude after attaining 25 cycles when compared to the first cycle. At still higher cycles, the rate of oxidation remained nearly constant.

3.2 Threshold thickness contributing to failure of integrity of scale

The integrity of the oxide scale is influenced both by growth stress and thermal expansion differential between the scale and the alloy. The latter factor plays a major role in disrupting the scale when the specimen is

subjected to thermal variations. Such is the case when the specimen is cooled after oxidation. The following discussion based on the present experiment is aimed at shedding light on the integrity of the scale vis-a-vis the thickness it has achieved.

(i) On oxidising at 1073 K, the scale appeared to be adherent even after completing 360 ks (100 h). The scale achieved a thickness of 15.58 μm at the end of 360 ks (100 h) oxidation.

(ii) On oxidising at 1123 K, the cracking of the scale was detected at the first cycle itself. The thickness of the cracked scale was 4.21 μm. The temperature of cracking was 606 ± 5 K in the cases of all the cycles .

(iii) The oxidation at 1173 K resulted in both cracking and spallation. The threshold thickness for the spallation of the scale was 108 μm. The spallation occurred on cooling to a temperature of 781 ± 5 K in the cases of all the cycles.

By a comparison of the above set of data, it is estimated that cracking of the oxide scale would have occurred even on oxidising at 1073 K. The dimensions of the crack and the associated mass gain are too small to be detected by the "transient mass gain" method which was employed to detect the integrity of the scale. Thus, from the present set of experiments, the following conclusions are drawn with respect to the adherence of the scale.

Threshold thickness for the cracking of the scale = 4.21 μm

Threshold thickness to initiate spallation = 108 μm

It should, however, be understood that the concept of threshold thickness is only a guiding parameter and is strongly dependent on experimental conditions such as heating rate, cooling rate and creep of the specimen.

In attempting to predict the total corrosion loss and the remnant life, it is not possible to provide absolute guidelines based on one set of experiments. The critical parameter contributing to failure of the scale must be understood and replicated in the experiment to facilitate near accurate evaluation of reduction in thickness and the remnant life.

The critical thickness for the failure of the scale depends on numerous factors including the intrinsic adherence capacity of the scale to the substrate, creep strength of the substrate material and operational parameters (cooling rate, cycle frequency etc.). Thus, the value of threshold thickness is only an indication regarding the corrosion rate likely to be experienced by the component. Spallation characteristics can vary from material to material and should not be exclusively related to achieving a particular thickness /17,18/. The possibility of relieving growth stress greatly influences the propensity to failure /19/. One general factor influencing the integrity of the scale is the thermal cycling and even extremely adherent scale tends to fail under this condition.

3.3. Nature of oxide phases

The oxides generated on the surface of the specimen (both retained and spalled) were analysed by X-ray diffraction by employing copper K-alpha as the incident source. The patterns obtained are given in Figs. 1, 2, 3, 4 and 5. The phases identified are summarised in Table 3.

Table 3

Oxide phases generated on cyclic oxidation of P91

History of specimen	Oxide phases identified
Oxidised for 360 ks (100 h) at 1073 K	Fe_2O_3, $FeCr_2O_4$ and Cr_2O_3
Oxidised for 360 ks (100 h) at 1123 K	$FeCr_2O_4$, Fe_2O_3
Oxidised for 360 ks (100 h) at 1173 K	$FeCr_2O_4$, Fe_2O_3
Oxide scales spallen from 1173 K specimen during oxidation	Fe_2O_3, $FeCr_2O_4$
Oxide scales spallen from 1173 K specimen at the end	Fe_2O_3, $FeCr_2O_4$

From the above data a possible mechanism for the oxidation process is explained as under.

Among the major constituents of mod. 9Cr-1Mo steel (iron and chromium), the oxide of chromium is thermodynamically more stable than that of iron. When this alloy is heated to high temperature in air, the oxides of both these elements are formed, as kinetics rather than thermodynamics dictates the course of the reaction.

Thus, a surface coating of Cr_2O_3, Fe_2O_3 or the mixed spinel is formed on the surface region that is exposed to the ambient air. On the other hand, the inter-space between the alloy and the oxide would experience a much lower partial pressure of oxygen. The continued growth of oxide scale at the inter-space (by the action of the metallic ions diffusing into the inter-space from the matrix) will bring down the partial pressure of oxygen to further lower level so that the oxide of iron is no longer stable. Such a process would lead to the formation of only Cr_2O_3 or $FeCr_2O_4$ at the inter-space.

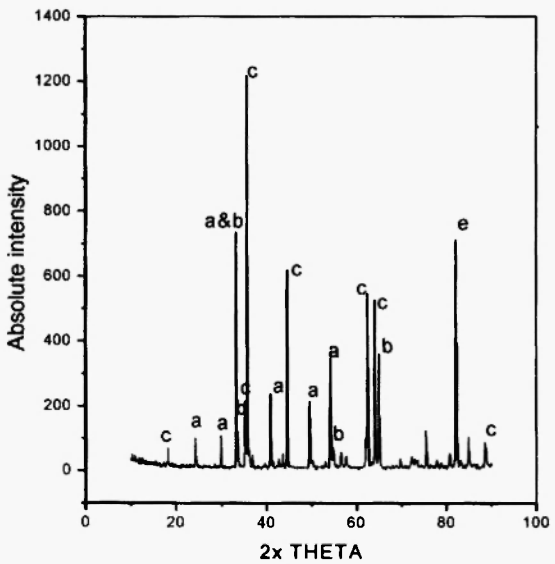

Fig. 1: XRD pattern of the surface of the specimen oxidised at 1013K (a = Fe_2O_3, b = Cr_2O_3, c = $FeCr_2O_4$, e = Ferrite phase)

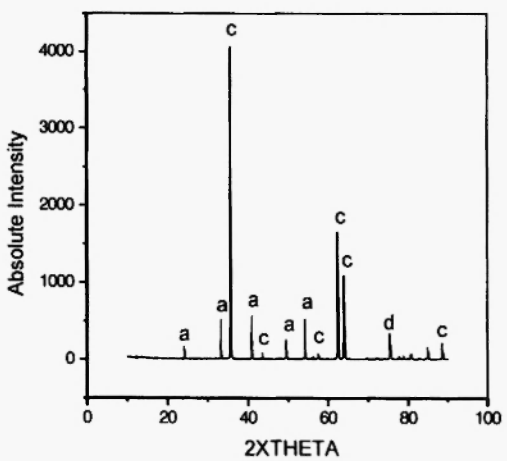

Fig. 2: XRD pattern of the surface of the specimen oxidised at 1123K (a=Fe_2O_3, c=$FeCr_2O_4$, d= FeO)

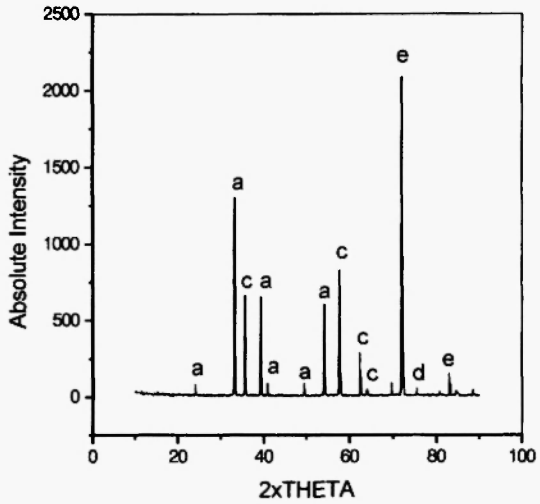

Fig. 3: XRD pattern of the surface of the specimen oxidised at 1173 K (a= Fe_2O_3, c=$FeCr_2O_4$, d=FeO, e=Ferrite phase)

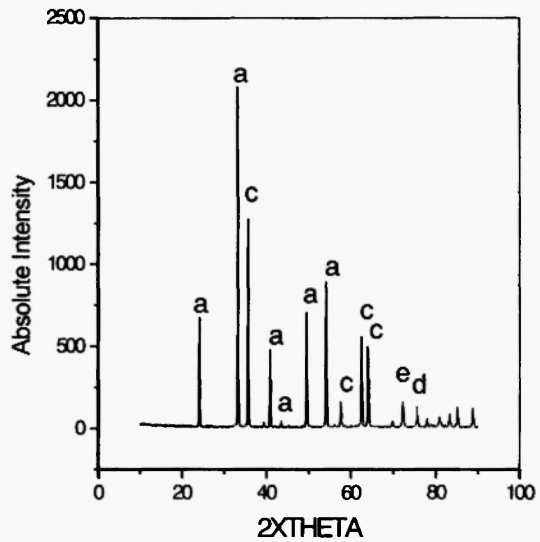

Fig. 4: XRD pattern of the spallen oxide (during experiment) of the specimen oxidised at 1173K (a = Fe_2O_3, c = $FeCr_2O_4$, d = FeO, e = Ferrite phase)

The growth of the oxide phase at the surface (leading to thickening of the scale) is determined by the rate of diffusion of cation through the pre-existing scale. The rate of diffusion of iron through the oxide scale is faster than that of chromium. Therefore the surface

oxide will be predominantly of iron and its spinel with chromium oxide.

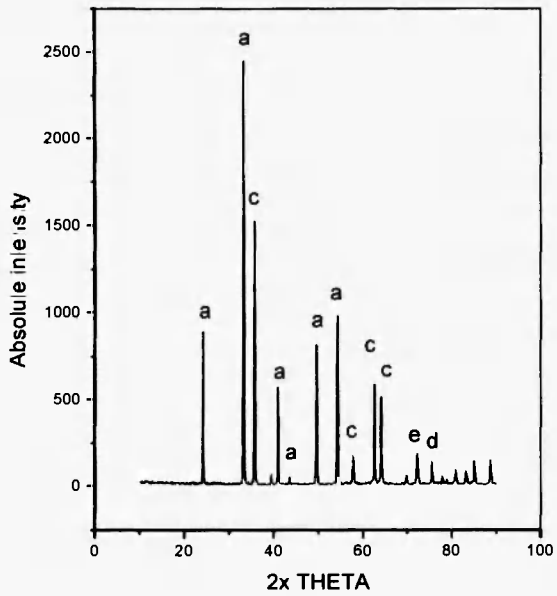

Fig. 5: XRD pattern of the spallen oxide (during handling) of the specimen oxidised at 1173K (a =Fe_2O_3,c=$FeCr_2O_4$, d = FeO, e = Ferrite phase)

At relatively lower temperature (1073 K in the present case), the amount of iron reaching the surface is not adequate to form exclusively oxide of iron. Thus, at least part of the chromium oxide, initially generated, is retained at the surface even after 360 ks (100 h) of oxidation. On the other hand at higher temperatures of 1123 and 1173 K the chromium oxide formed initially is pushed to the interior (due to the outward growth of the scale) and the outside layer is completely of iron oxide or spinel.

The above mechanism is further substantiated by the XRD analysis of the oxide scale spallen from the specimen oxidised at 1173 K. The spallen oxides completely consisted of Fe_2O_3 and $FeCr_2O_4$. Analysis of the spalled region by EDS revealed the generation of oxide of chromium which is explained in a later section.

3.4 Surface morphology by scanning electron microscopy

Surface morphology of the oxide scale was examined using scanning electron microscope. This investigation was carried out at the end of 25 cycles and 50 cycles. The micrographs are shown in Figs. 6, 7 and 8.

The specimen oxidised at 1073 K for 25 cycles [(Fig 6(a)] showed the development of fine grained oxide precipitate, uniformly spread on the surface devoid of any crack. At the end of 50 cycles [Fig 6(b)], nodular structure was developed on the surface. Here again there was no development of cracks or buckling of the scale.

The specimen oxidised at 1123 K, showed a marked difference of behaviour. The oxide scale showed

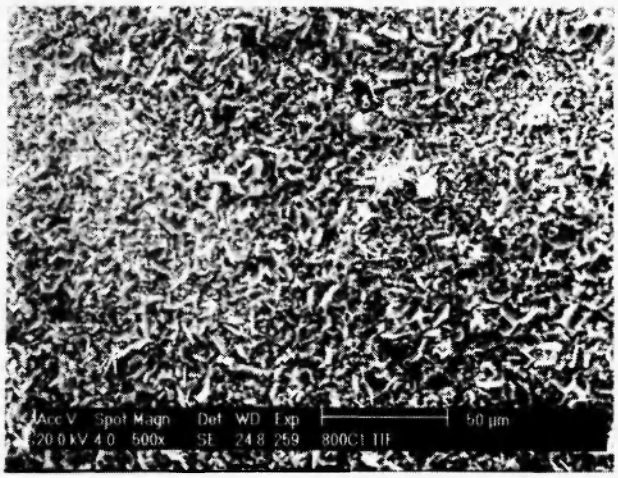

(a)

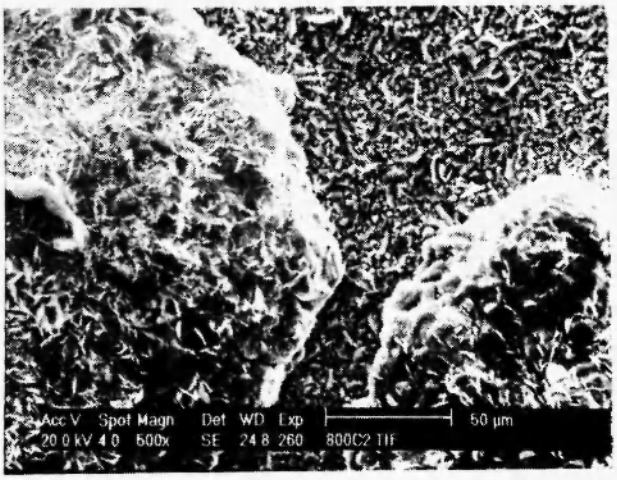

(b)

Fig. 6: Scanning Electron Micrograph of the surface of P91 oxidised at 1073 K; (a) after 25 cycles (180 ks, 50 h) (b) after 50 cycles (360 ks, 100 h)

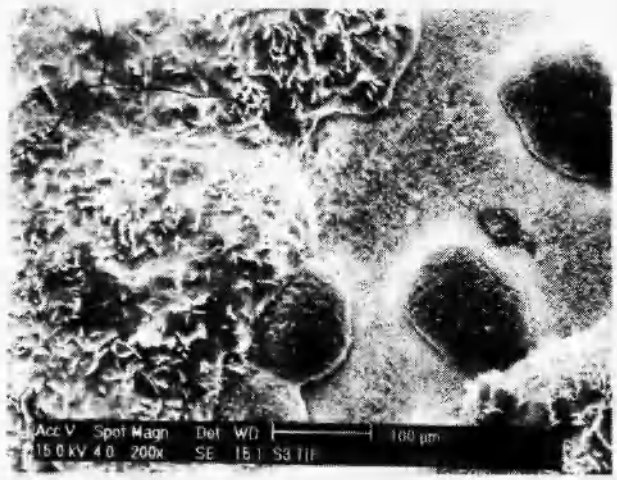

(a)

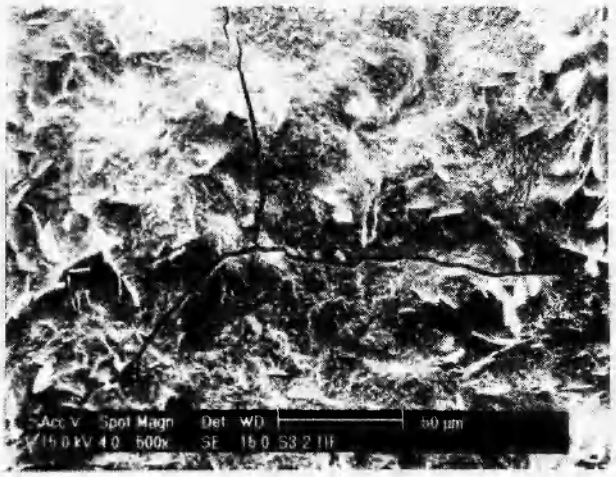

(b)

Fig. 7: Scanning Electron Micrograph of the surface of P91 oxidised at 1123 K; (a) after 25 cycles (180 ks, 50 h) (b) after 50 cycles (360 ks, 100 h)

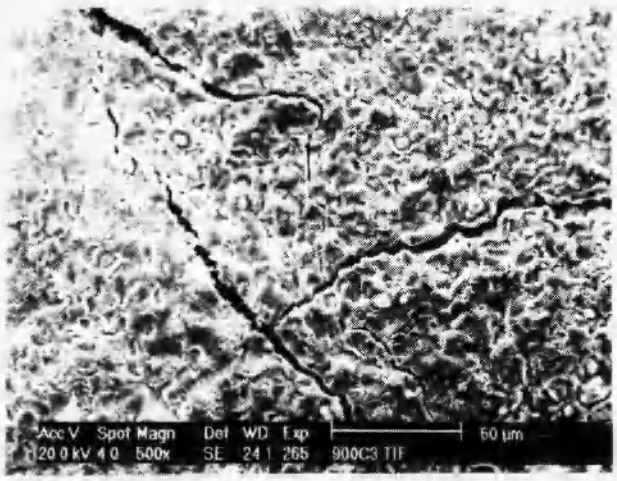

(a)

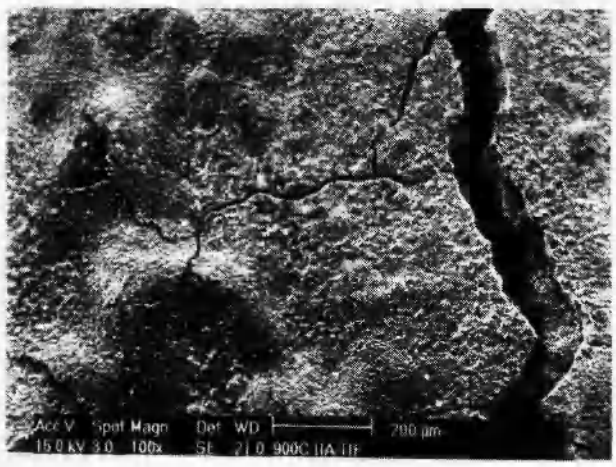

(b)

Fig. 8: Scanning Electron Micrograph of the surface of P91 oxidised at 1173 K; (a) after 25 cycles (180 ks, 50 h) (b) after 50 cycles (360 ks, 100 h)

tendency to sintering and the nodular growth was further distinct when compared to the specimen oxidised at 1073 K. At the end of 25 cycles itself cracks were seen on the surface [Fig 7(a)]. These cracks were not grown enough to cause spallation. On completing 50 cycles, the cracks were further enlarged, but still short of initiating a spallation [Fig. 7(b)].

On oxidising at 1173 K, the oxide scale showed enhanced sintering characteristics. The oxide scale was completely deprived of fine-grained structure. Cracks were observed at the end of 25 cycles itself [Fig 8(a)] that further aggravated at the end of 50 cycles [Fig 8(b)]. The cracks were interconnected to promote spallation. Cracks were generated on oxidising the specimen itself and spallation was considerably aggravated on handling of the specimen for post-oxidation examination.

3.5. Analysis of the oxidised surface by Energy Dispersive Spectrometry (EDS)

The analytical results of the scale are given in Table 4. The uniform region of the scale on the specimen that was oxidised at 1073 K contained 30.81% Fe and 69.19% Cr in the oxide scale. Thus, the scale is predominantly comprised of the oxide of chromium. On the other hand, the nodular region of the same specimen contained predominantly iron oxide (96.4% Fe and 3.6 % Cr)

The specimen oxidised at 1123 K exhibited a different picture. Both the uniform region and nodular region consisted predominantly of oxide of iron. In the uniform region the composition of the scale was 97.02% Fe and 2.98 % Cr and in the nodular region it was 98.7% Fe and 1.23 % Cr. This observation adds credence to the proposal that at higher temperature more ions of iron reach the surface by diffusion through the pre-existing scale.

On oxidising at 1173 K, the uniform layer comprised of two distinct regions of small crystallite and large crystallite. The large crystallite was found to consist of only iron oxide. The small crystallite contained a small fraction of chromium oxide (97.4 % Fe and 2.58 % Cr). The spalled region showed a relative increase in the content of chromium oxide. Two such regions were analysed. The content of oxides were 93.6 % Fe and 6.4 % Cr underneath the first spalled region. The corresponding concentrations of iron and chromium in the second spalled region were 84.9 % Fe and 15.1 % Cr. These analytical results further support the mechanism proposed in section 3.3 to explain the oxide growth.

The presence of higher concentration of chromium oxide and spinel at the spalled regions is attributed to the very low oxygen pressures present in the inter-spaces of the oxide and the alloy. At very low pressures of oxygen the oxide of chromium is more stable than that of iron. However, analysis by XRD could not indicate the presence of Cr_2O_3 because the concentration was too low to be determined by this method.

Table 4
Composition of the oxide phases formed on the specimens

Temperature of oxidation/ K	Region of the surface analysed	Composition
1073	Uniform region	30.81%Fe, 69.19%Cr
"	Nodular region	96.4%Fe, 3.6%Cr
1123	Uniform region	97.02%fe, 2.98%Cr
"	Nodular region	98.77%Fe, 1.23%Cr
1173	Small crystallite	97.42% Fe, 2.58%Cr
"	Big crystallite	100%Fe
"	Spalled region I	93.6%Fe, 6.4%Cr
"	Spalled region II	84.9% Fe,15.1%Cr

4. CONCLUSIONS

Specimens of modified 9Cr-1Mo steel were subjected to cyclic oxidation at temperatures of 1073, 1123 and 1173 K. Experiments have indicated that the integrity of the scale is significantly affected due to thermal cycling and only marginally while maintaining at the respective temperatures of oxidation. This behavior is attributed to the large difference in the thermal expansion coefficients between the oxide and the alloy. Both cracks and spallation occur after the oxide scale has attained a definite thickness. This value has been estimated by the present experiment and given as under:

Threshold thickness for cracking of the scale = 4.21 μm

Threshold thickness for spallation = 108 μm

The threshold thickness depends on several experimental variables and hence should be taken only as an indicative parameter. For the actual components in the service environment, the failure of the scale will be influenced by several physicochemical and mechanical factors. However, such data are very valuable for inter-comparison of the relative performance of various alloys and to assist the designer in accounting for the oxidation loss likely to occur during the life of a component.

The oxide phase generated at the surface is predominantly Fe_2O_3 and $FeCr_2O_4$ at 1123 and 1173 K. A small fraction of Cr_2O_3 was also observed at the surface of the specimen oxidised at 1073 K. The interspace of the oxide and alloy was also found to consist of significant amounts of Cr_2O_3. Such a behaviour of oxide scale distribution is accounted by the faster diffusion of iron through pre-existing scale so that predominantly the oxide of iron and spinel is generated at the surface. The partial pressure of oxygen at the interspace of the scale is too low so that the oxide of chromium was also formed.

5. ACKNOWLEDGEMENT

The authors wish to acknowledge Dr. V. Sankara Sastry, Materials Science Division of this Organization, for his valuable help in XRD analysis. The authors are also thankful for the support and encouragement provided by Dr. V.S. Raghunathan, Associte Director, Materials Characterization Group of this organization.

6. REFERENCES

1. F.A. Golightly, F.H. Stott and G.C. Wood, *Oxid. Met.* **10**, 163 (1976).
2. I.A. Allam, D.P. Whittle and J. Stringer, *Oxid. Met.* **13**, 381 (1978).
3. C.S. Giggins, B.H. Kear, F.S. Petit and J.K. Tien, *Metall. Trans.* **5**, 1685 (1974).
4. T.A. Ramanarayanan, M. Raghavan and R. Petkovic Luton, *J. Electrochem Soc.* **131**, 923 (1984).
5. L. Singheiser, R. Steinbrech, W. J. Quadakkers and R. Herzog, *Mater. High Temp.* **18**(4), 193 (2001).
6. A.G. Evans, G.B. Grumbley and R.E. Demarey, *Oxid. Met.* **20**, 193 (1983).
7. A. Rahmel and M. Schuetze, *Oxid. Met.* **38**, 255 (1992).
8. M. Schuetze, *Oxid. Met.* **24**, 199 (1985).
9. M. Schuetze, *Protective Oxide Scales and their Breakdown*, J. Wiley and Sons, Chichester, U.K. 1997
10. R. Mevrel, *Mater. Sci. Technol.* **3**, 531 (1987).
11. S. Rajendran Pillai, N. Sivaibarasi and H.S. Khatak, *Oxid. Met.* **54**, 211 (2000).
12. H.E. Evans, *Intern. Mater. Rev.* **40** (1), 1 (1995).
13. J.L. Smialek, J.A. Nesbitt, C.A. Barrett and C.E. Lowell, in: *Cyclic Oxidation of High Temperature Materials*, Eds. M. Schuetze and W.J. Quadakkers, European Federation of Corrosion, Publication No. 37 IOM Communication, 1999; p. 148
14. J. L. Smialek, *Metall. Trans.* **9A**, 309 (1978).
15. W.J. Quadakkers and M.J. Bennet, *Mater. Sci. Technol.* **10** (2), 126 (1994).
16. U. Krupp and H.-J. Christ, *Oxid. Met.* **52**, 277 (1999).
17. W.J. Quadakkers and K. Bongartz, Werk. *Korros.* **45**, 232 (1994).
18. H.E. Evans, *Mater. High Temp.* **12**, 219 (1994).
19. Krishan L. Luthra and Clyde L. Briant, *Oxid. Met.* **26**, 397 (1986).